Dynamic modeling and sensitivity analysis of perlite grain expansion in a vertical electrical furnace

DYNAMIC MODELING AND SENSITIVITY ANALYSIS OF PERLITE GRAIN EXPANSION IN A VERTICAL ELECTRICAL FURNACE

Panagiotis M. Angelopoulos[1*], Dimitrios I. Gerogiorgis[2], and Ioannis Paspaliaris[3]

Laboratory of Metallurgy
School of Mining and Metallurgical Engineering
National Technical University of Athens
Athens, GR-15780, Greece

e-mail: [1] pangelopoulos@metal.ntua.gr, [2] dgerogiorgis@metal.ntua.gr, [3] paspali@metal.ntua.gr

Keywords: Perlite expansion, vertical electrical furnace, process design, dynamic modeling, sensitivity analysis

Abstract. *Expanded perlite has outstanding thermal and acoustic insulating properties and is widely used in the manufacturing and construction industries. The conventional perlite expansion method suffers disadvantages which affect the quality of expanded perlite products, thus limiting their performance and range of applications. A new perlite expansion process has been designed and a vertical electrical furnace for perlite expansion has been constructed in our laboratory in order to overcome these drawbacks, enabling precise control of experimental conditions, so as to prescribe the temperature profile and residence time in the heating chamber. Perlite ore origin, size distribution and water content are critical parameters affecting expanded perlite quality; air feed flow rate and temperature, as well as the imposed wall temperature distribution along the chamber are also experimentally known to have a profound, measurable effect on perlite grain residence time and expansion. A detailed sensitivity analysis has been performed in order to quantitatively understand the effect and relative importance of all these operational parameters on macroscopic furnace operation (perlite particle velocity and temperature evolution) and inaccessible microscopic characteristics (internal steam bubble pressure and size), based on a new dynamic model for perlite grain expansion we have developed towards furnace optimization [1].*

1 INTRODUCTION

Perlite is a natural occurring volcanic siliceous rock which consists mainly of amorphous silica (70-76 % wt.) but also contains smaller quantities of numerous other metal oxides (Al_2O_3, K_2O, Na_2O, Fe_2O_3, CaO, MgO). Perlite can be expanded from 4 to 20 times its original volume when heated at a temperature close to its softening point (700-1260 °C), due to the presence of 2-6% chemically bound water within its microstructure [2]. Conventional perlite expansion is usually accomplished by feeding ground, pre-sized perlite ore into a vertical furnace heated by a direct gas flame at its bottom end, thus directing forced air flow upwardly: ore particles are typically introduced into the hottest expansion chamber region, near the flame, at a temperature of 1450 °C [3]. During expansion, perlite acquires outstanding physical properties (e.g. low density, thermal and acoustic insulation) which render it suitable for numerous applications in the construction and manufacturing industries. The currently prevalent perlite expansion process is virtually the only globally reliable production method: although it has been in continuous use for more than 50 years, it remains a largely empirical industrial process, despite the rapid increase and proliferation of expanded perlite uses and applications over the past few decades. Its main technical problems include the increased heat losses due to the off-gas stream, leading to high energy consumption, but also the violent and poorly controlled heating of perlite which results in an expanded material with unfavourable mechanical properties, which adversely affect quality and limit the range of its applications.

To overcome these drawbacks, a novel perlite expansion process has been designed and a new pilot-scale production unit has been constructed, based on the concept of a vertical, electrically heated expansion furnace. The new vertical electrical furnace has been designed for maximizing experimental flexibility, in order to facilitate the adjustment of operating conditions versus raw material but also final product quality specifications. The new perlite expansion method allows the milder, gradual heating of perlite grains, as well as the variation of perlite grain residence time in the heating chamber. Experimental perlite expansion campaigns conducted on this pilot-scale production unit indicate a remarkable improvement as well as a definite operating cost reduction in expanded perlite properties compared with conventional processing. Hence, the multi-parametric mathematical investigation of the process system thermal behavior and the identification of the effect of all crucial operational parameters on perlite expansion dynamics is an endeavor of evident importance which must guide the eventual optimization of the entire pilot-scale experimental facility and every subsequent production-scale process. Investigating the effect of key operational parameters on product quality yields profound process understanding.

2 THE VERTICAL ELECTRICAL FURNACE CONFIGURATION AND OPERATION

2.1 Vertical electrical perlite expansion furnace

The vertical electrical perlite expansion furnace consists of the air preheater and flow control system, the perlite feeding system, the heating chamber and the furnace temperature control system (Figure 1). Atmospheric air is introduced into the system by an air compressor and the volumetric flow rate is measured and controlled by a dedicated system of flowmeters and valves. The air is injected at the top of the furnace through six 0.009 m-diameter holes located symmetrically around the perlite inlet hole and at a distance of 0.044 m from the center. Air can be heated by a preheater which has a heat capacity of 2 kW and can raise temperature to up to 450 °C. The desirable perlite feeding rate is achieved by a rotary air-lock feeder, through a 0.08 m diameter central hole. The rotary air-lock feeder prevents hot air upward drafts but also the escape of perlite particles from the furnace.

The cylindrical heating chamber is 3 m long and 0.134 m wide, and is made of Kanthal APM FeCrAl alloy. The chamber is heated by 6 pairs of electrical resistances located along the tube, defining six heating zones. Each pair consists of two semicylindrical Kanthal resistances, located against each other around the chamber and at a distance of about 3 cm out of it, providing a total heating capacity of 24 kW to the expansion process. The chamber and resistances are encased in a cylindrical alunimosilicate insulation case of 0.165 cm thickness. Temperature measurements within each thermal zone are obtained via a ceramic sheathed K-type thermocouple (NiCr/NiAl) placed at each zone center; air inlet temperature is measured by a thermocouple located before the furnace head. Preheater as well as heating zone temperatures can all be individually controlled by the operator.

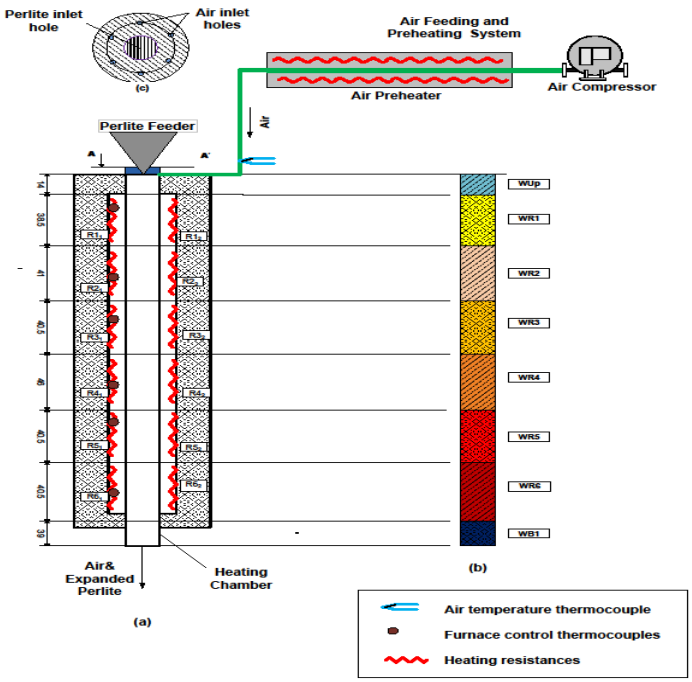

Figure 1. Schematic of the prototypic experimental installation constructed at NTUA for perlite expansion, illustrating the vertical electrical furnace and head layout, its 6 electrical heating zones and all auxiliary systems.

2.2 Dynamic mathematical modeling assumptions

The fundamental assumptions for developing the macroscopic and microscopic parts of the mathematical model are important in order to understand the scope and accuracy of the model as well as the limits of its applicability. Air is introduced through the entire face of the cylindric chamber, without any pressure drop (P = 1 atm): its temperature along the heating chamber has no radial variation, and the entire chamber wall surface is smooth. Air temperature and velocity distributions are studied via one-dimensional models, as radial air velocity is zero. The effect of air components which are not transparent to thermal radiation (CO_2, H_2O) is negligible and does not affect air heating. Each perlite grain is considered perfectly spherical throughout the expansion process, and has a uniform temperature which varies during expansion only because of heating and evaporation phenomena. Perlite shell melt, thermal conductivity and specific heat capacity are considered constant throughout expansion. Diffusion or mass transfer across the bubble-shell and the shell-environment interface has not been considered. The entire amount of the effective water content within the perlite grain is concentrated at the steam bubble nucleus throughout the expansion process. Steam obeys the ideal gas law in the entire process. The enthalpy of water evaporation inside grains is explicitly considered, but mechanical work for bubble expansion is negligible.

3 AIR AND PERLITE MELT PROPERTIES

3.1 Air thermophysical properties

Air can be injected into the heating chamber at a temperature of 25 °C and heated up to 1200 °C: property variations are expected to be dramatic, so incorrect estimates induce significant error in energy balance models. The estimation of a mean air temperature in the heating chamber is used for air transport property calculations:

$$T_{mean} = \frac{T_{air,in} + T_w}{2} \tag{1}$$

Here, T_{mean} is the mean air temperature, while $T_{air,in}$ and T_w are the air temperature at the inlet of the furnace and the heating chamber wall temperature (both in K), respectively. The air density variation affects the volumetric air flow rate along the vertical heating chamber, inducing an increase of superficial air velocity; it also affects the buoyancy and drag forces on perlite grains and the convective heat transfer rate from the air to the particle. Air density variation along the vertical heating chamber is calculated by the ideal gas law constitutive equation:

$$\rho_{air} = \frac{P}{R_g T_{air}} \tag{2}$$

Here, ρ_{air} is the air density (kg·m^{-3}), R_g is the ideal gas law constant and pressure is taken constant (P = 1 atm). The model assumes constant air dynamic viscosity (μ_{air}), heat capacity (k_{air}), thermal conductivity (C_{Pair}) and Prandtl number (Pr_{air}) at mean temperature. Air dynamic viscosity has been calculated using the next equation:

$$\mu_{air} = \mu_{air,ref}\left(\frac{T_{air,mean}}{T_{air,ref}}\right)^{n_{ref}} \tag{3}$$

Parameter values for air viscosity calculation are: $\mu_{air,ref}$ = 1.72·10^{-5} Pa·s, $T_{air,ref}$ = 273 K, n_{ref} = 0.7, respectively.

$$C_{p,air} = \alpha_{C_p,1} T_{air,mean}^{\ 3} + \alpha_{C_p,2} T_{air,mean}^{\ 2} + \alpha_{C_p,3} T_{air,mean} + \alpha_{C_p,4} \tag{4}$$

Coefficient values for $\alpha_{C_p,1}, \alpha_{C_p,2}, \alpha_{C_p,3}, \alpha_{C_p,4}$ are: -8.01440·10^{-8}, 2.10788·10^{-4}, 2.06329·10^{-2}, 9.83672·10^{2}, respectively.

$$k_{air} = \alpha_{k,1} T_{air,mean}^{\ 3} + \alpha_{k,2} T_{air,mean}^{\ 2} + \alpha_{k,3} T_{air,mean} + \alpha_{k,4} \tag{5}$$

Coefficient values for $\alpha_{k,1}$, $\alpha_{k,2}$, $\alpha_{k,3}$, $\alpha_{k,4}$ are: -1.5207·10^{-11}, -4.8574·10^{-8}, 1.0184·10^{-4}, -3.9333·10^{4}, respectively. Figure 2 presents all foregoing air thermophysical properties involved in the dynamic model (ρ_{air}, μ_{air}, C_{Pair}, k_{air}) which have been calculated by the aforementioned equations in the entire temperature range of process interest.

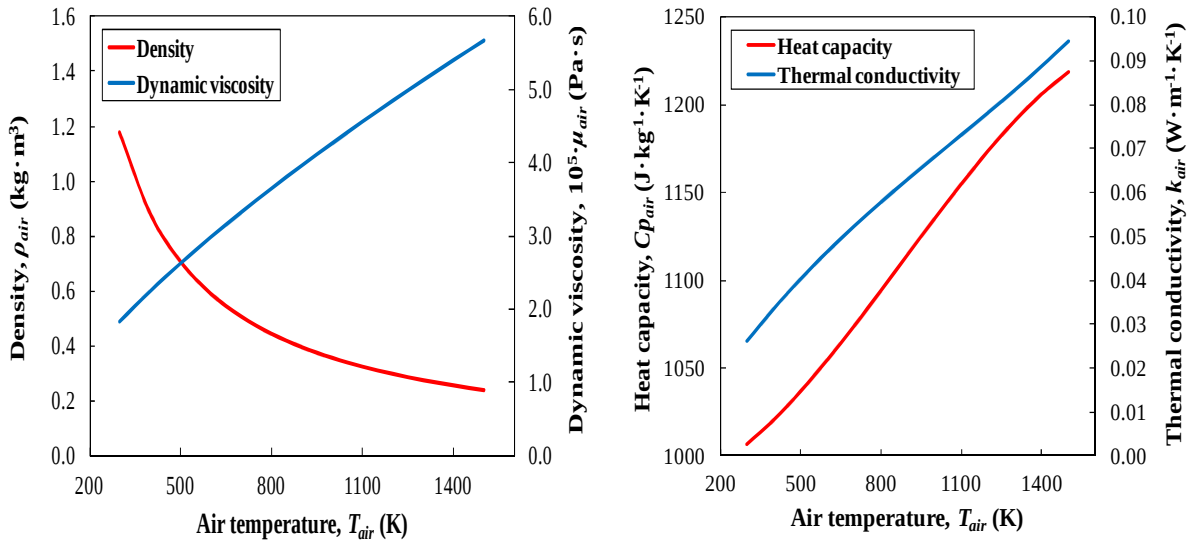

Figure 2. Air thermophysical properties as a function of temperature over the entire range of process interest.

3.2 Perlite melt thermophysical properties

Perlite ore particles from the Trachilas (TR) and Tsigrado (CH) mines (Milos island, Greece) have been studied. The perlite ore considered in this modeling study consists of amorpous silica (73% wt. SiO_2), aluminium oxide (12.7% Al_2O_3), other metal oxide amounts (K_2O, Na_2O, Fe_2O_3, CaO) and 3.32 % LOI (Lost On Ignition) matter. Water plays the most important role during the entire expansion process, not only by expanding the grain during evaporation but also by reducing the viscosity of the softened grain shell; the amount of perlite water which is available and responsible for its potential to expand on heating has been studied by previous publications [4][5]. Based on LOI tests, we conclude that a water portion remains in the expanded grain without participating in expansion: this is the *residual water* (40%) which is only considered in perlitic melt thermophysical property calculation, while the remaining *effective water* (60%) drives steam bubble growth and perlite grain expansion. Perlite melt density is assumed constant (ρ_m = 2300 kg·m^{-3}) in the entire grain temperature range; Zahringer *et al.* used a mean value of 2350 kg·m^{-3}, while Proussevitch *et al.* used a rhyolitic melt density of 2200 kg·m^{-3} [6][7]. Our raw perlite ore density measurement (2290 kg·m^{-3}) agrees with melt density values reported in the literature.

Perlite expansion evolution is affected by molten grain shell viscosity, which varies significantly during the process and is a strong function of temperature: in a relevant publication, Giordano *et al.* studied compositional and temperature effects on magmatic liquid viscosity, developing a multi-parametric algebraic model which is used here and calculates melt viscosity as a function of both chemical composition and absolute temperature [8]. The temperature dependence of viscosity is accounted for by the Vogel-Fulcher-Tammann (VFT) equation [9][10], with J, X and Y (pre-exponential factor, pseudo-activation energy and VFT temperature, respectively) all given:

$$\log \mu = J + \frac{X}{T_m - Y} \tag{6}$$

The surface tension exerted on the shell-bubble interface is crucial, since it counteracts bubble expansion. The temperature dependence of perlitic melt surface tension (σ) can be approximated by a published correlation for obsidian melt (0.5% wt. H_2O). The equation which is presented below is valid in the 1000-1400 °C range [6]:

$$\sigma = 0.09317 + 1.971 \cdot 10^{-4} \mathrm{T}_m \tag{7}$$

Figure 3 presents the variation of perlite melt thermophysical properties (melt viscosity and surface tension). Perlite melt viscosity decreases dramatically (by several orders of magnitude) with increasing melt temperature; it also decreases considerably (by at least one order of magnitude) with increasing water content (0.5-2.0%). Ambient to low-temperature melt viscosity (within the 297-973 K temperature range) is extremely high, thus hindering shell softening and particle expansion completely, as explained by the bubble radius equation (22). Perlite melt water content is a critical parameter which greatly affects the melt viscosity: considering the strong dependence of molten shell softening (cause) and particle expansion (effect), this explains the vastly different experimental results that are routinely obtained for only slightly different (less than 1% H_2O) raw perlite feeds. The multi-parametric literature model of Giordano et al. [8] used here captures and confirms these observations. The surface tension of obsidian is similar to perlite and increases linearly with increasing melt temperature [8].

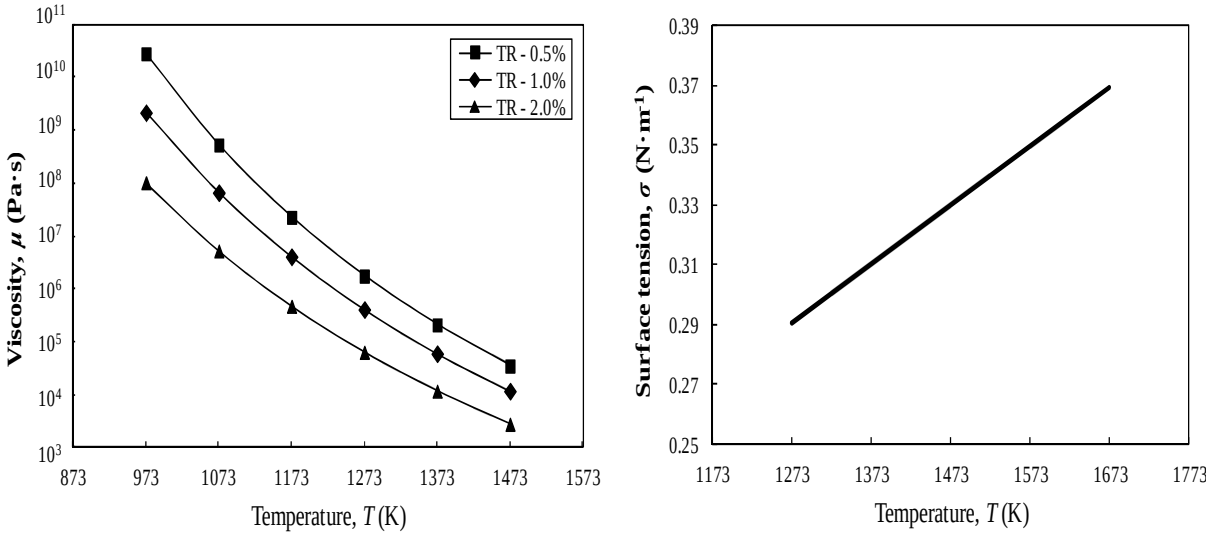

Figure 3. Melt viscosity as a function of temperature and water content for three Trachilas (TR) perlite samples calculated via a literature model [8] (left). Obsidian melt surface tension as a function of temperature [6] (right).

4 THE MATHEMATICAL MODEL

The dynamic mathematical model which we have developed concentrates on the momentum and energy balance description of single-grain expansion in the vertical electrical furnace, at a microscopic and a macroscopic level. Microscopic mathematical analysis here refers to the investigation of internal particle temperature and steam bubble pressure evolution, as the interplay and rates of both these phenomena governs perlite grain expansion. Macroscopic mathematical analysis refers to particle motion (force balance) and air temperature distribution. These transport phenomena are analyzed via a nonlinear system of algebraic and ordinary differential equations.

4.1 Perlite particle motion along the vertical heating chamber

The forces exerted on the falling particle are the gravitational force (F_G) which accelerates the particle, the drag force (F_D) and the buoyancy force (F_B) which decelerate the perlite grain vertical fall by opposing its motion:

$$F_g = m_p g \qquad (8) \qquad F_D = \frac{1}{2}\rho_{air} C_D A_{proj} \left(U_{air} - U_p\right)^2 \qquad (9) \qquad F_B = \rho_{air} g V_p \qquad (10)$$

The momentum balance on the falling perlite particle follows Newton's second law of mechanics: considering all forces exerted on a grain, the particle velocity evolution is calculated by an ordinary differential equation[11]:

$$\sum F = m_p \frac{dU_p}{dt} \Rightarrow \frac{dU_p}{dt} = \frac{\rho_p - \rho_{air}}{\rho_p} g - \frac{3}{4}\frac{\rho_{air} C_D \left(U_{air} - U_p\right)^2}{d_p \rho_p} \qquad (11)$$

The drag force coefficient (C_D) is calculated via a correlation based on the particle Reynolds number (Re_p) [11] :

$$C_D = \frac{K_1}{\mathrm{Re}_p} + \frac{K_2}{\mathrm{Re}_p^2} + K_3 \qquad (12)$$

The particle Reynolds number (Re_p) is calculated based on the relative velocity by the following equation [12]:

$$\mathrm{Re}_p = \frac{\rho_{air} d_p \left|U_p - U_{air}\right|}{\mu_{air}} \qquad (13)$$

The volumetric air flow rate due to the increase of air temperature and the decrease of air density along the grain trajectory in the heating chamber is taken into account toward air velocity calculation by the following equation:

$$U_{air} = \frac{\dot{Q}_{air,in} T_{air}}{A_{tube} T_{air,in}} \qquad (14)$$

4.2 Air heat balance in the vertical heating chamber

The problem of air temperature calculation in the heating chamber can be considered and solved as follows: air is injected into a vertical tube and flows at mean velocity, within heated furnace walls of constant temperature. Thermal energy is transferred to the fluid (air) by convection, thereby causing an increase in the air temperature. Air temperature calculation is based on an adiabatic energy balance, with the initial condition T_{air} (t = 0) = $T_{air, in}$.

$$\frac{dT_{air}}{dt} = \left(\frac{\pi d h_{mean}}{\dot{m} C_{p_{air,mean}}}\right)\left(T_w - T_{air}\right) \qquad (15)$$

The mean convective heat transfer coefficient (h_{mean}) therein is calculated by the following algebraic equation:

$$h_{mean} = \frac{k_{air} Nu_{mean}}{d} \qquad (16)$$

The mean Nusselt number along the heating chamber is calculated by Hausen's equation, which explicitly includes the effect of the thermal entry length, within which the heat transfer coefficient is not yet constant [13]:

$$Nu_{mean} = Nu_\infty + \left[\frac{0.104\left(\left(\frac{d}{L}\right)\mathrm{Re}_t\,\mathrm{Pr}_{air}\right)}{1 + 0.016\left(\left(\frac{d}{L}\right)\mathrm{Re}_t\,\mathrm{Pr}_{air}\right)^{0.8}}\right]\left(\frac{\mu_{air}}{\mu_w}\right) \qquad (17)$$

4.3 Perlite grain energy balance in the vertical heating chamber

The falling perlite grain is assumed to have a uniformly varying temperature, as internal gradients are negligible. The validity of this assumption is confirmed by a Biot number calculation for a compact unexpanded particle: for the thermophysical properties and conditions considered, one can numerically confirm that its value (*Bi*) does not exceed *Bi* = 0.047, even in the most unfavorable case of maximum resistance to conductive heating. As the maximum Biot number is much lower than the limit value of Bi_c = 0.1 (a case for which literature indicates that total radial temperature variation cannot exceed 5%), the uniform temperature assumption is valid.

The solid particle absorbs energy by radiation and convection: both contribute to heating and expansion and they are equally important heat transfer mechanisms in order to understand furnace as well as process efficiency. The grain temperature evolution due to radiative heating is calculated on the basis of the Stefan-Maxwell law, thus accounting for the thermal energy emitted by the furnace walls and absorbed by the moving perlite grain. Furthermore, the solid particle exchanges thermal energy with air by convective heating: this is an interesting phenomenon, as one can in fact numerically identify a sign reversal along the perlite grain trajectory: initially the cold particles are heated by the upward air current, but they are warmer than air as they approach the exit. Consequently, perlite grain temperature evolution is governed by the combination of radiative and convective heat transfer mechanisms and the dynamic heat balance is given by the following ordinary differential equation:

$$\frac{dT_p}{dt} = \varepsilon_w \cdot \frac{A_s s\left(T_w^4 - T_p^4\right)}{\rho_p V_p C_{p_p}} + \frac{A_s h_c \left(T_{air} - T_p\right)}{\rho_p V_p C_{p_p}} - \Delta H_{evap} \left(\frac{P_b}{R_g T_p}\right)\left(\frac{4\pi R_b^3}{3}\right) \tag{18}$$

Here, ε_w is the furnace wall emissivity (estimated at ε_w = 0.7 by construction) [14], A_s is the perlite particle surface area, *s* is the Stefan-Boltzmann constant and ΔH_{evap} is the molar enthalpy of water evaporation (40.68 kJ·mol^{-1}).

4.4 Steam bubble growth within the perlite grain

In the present mathematical modeling study, perlite expansion is approximated by a detailed single-grain model. The model particle consists of a spherical steam nucleus and a solid shell surrounding the steam bubble: steam is treated as an ideal gas, with no mass transfer across the steam-shell or the shell-environment interface permitted. During particle heating, the perlite grain temperature increase has a dual effect: firsly, steam enthalpy increases, thereby increasing the pressure exerted on the bubble-shell interface; concurrently, molten shell viscosity and cohesion decrease, thus facilitating bubble expansion and increasing steam bubble radius and perlite grain size.

The pressure factors acting on the bubble-shell interface are the surface tension (σ), the steam pressure (P_b), and the ambient pressure (P_a): steam pressure acts towards expanding the bubble, while both surface tension and ambient pressure act against steam bubble growth. The steam bubble only contains the entire effective water amount, since the residual water amount is uniformly dispersed in the molten shell without affecting expansion. The initial steam bubble radius ($R_{b,i}$) can be calculated by means of mass by the following algebraic equation:

$$R_{b,i} = \sqrt[3]{R_{p,i}^3 - \frac{3}{4\pi}\frac{m_m}{\rho_m}} \tag{19}$$

The molten shell mass (m_m) is calculated using the grain water mass fraction (w_{H2O}) by the following equation:

$$m_m = \left(1 - w_{H_2O}\right) m_p \tag{20}$$

The steam in the core of the grain is treated as ideal gas: its instantaneous pressure is calculated by considering the bubble radius evolution in the bubble volume term and implementing the ideal gas law constitutive equation:

$$P_b(t) = \frac{3NR_gT_p}{4\pi R_b^3(t)} \tag{21}$$

The Navier-Stokes equation for spherical creeping flow is combined with the melt radial velocity equation and the bubble surface stress balance, to yield an ordinary differential equation for bubble radius evolution [15][16][17]:

$$\frac{dR_b}{dt} = \frac{R_b}{4\mu_m}\left(P_b(t) - P_a - \frac{2\sigma}{R_b}\right) \tag{22}$$

The required initial condition is the miniscule steam bubble radius assumed at particle injection: $R_b(t = 0) = R_{b,i}$.

5 RESULTS AND DISCUSSION

A computer model has been developed so as to streamline the systematic numerical investigation of the process. The dynamic operation of the novel furnace is modeled using the Berkeley Madonna® ODE modeling platform (version 8.3.18), using a dual-core Intel Pentium T3200 (2 GHz) with 3 GB of RAM in Windows Vista (32-bit). The nonlinear system of algebraic and ordinary differential equations is solved using a 4th-order Runge-Kutta numerical integration method, using solution and reporting timesteps of $\Delta t_s = 0.01$ s and $\Delta t_r = 0.05$ s, respectively.

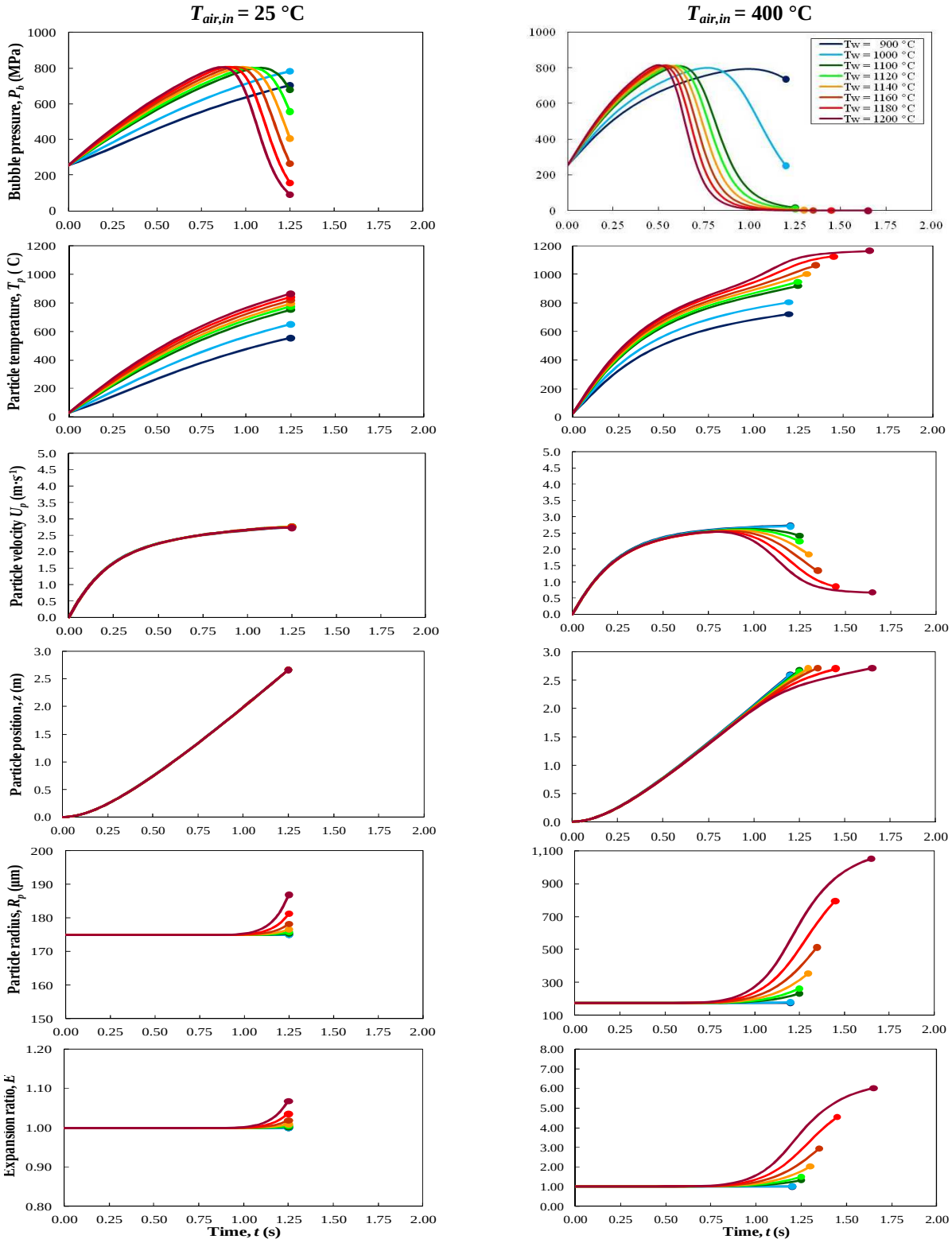

Figure 4. Temporal evolution of particle state variables as a function of heating chamber wall temperature, for the two air feed temperature extremes. Constant parameters: $Q_{air,in}$ = 50 L·m^{-1}, D_{pi} = 350 μm, $w_{H2O,eff}$ = 1.75%.

Figures 4 and 5 present all perlite particle state variables for various furnace wall temperatures and for particle effective water content: $w_{H2O,eff}$ = 1.75% (Tsigrado/CH sample) and $w_{H2O,eff}$ = 2.00% (Trachilas/TR sample). Particle pressure increases with increasing perlite grain temperature: a clear relief occurs when T_p = 600 °C, indicating the point where shell viscosity and cohesion decrease enough in order to trigger bubble expansion. Particles decelerate rapidly at expansion onset, due to the strong radius impact on the drag and buoyancy forces.

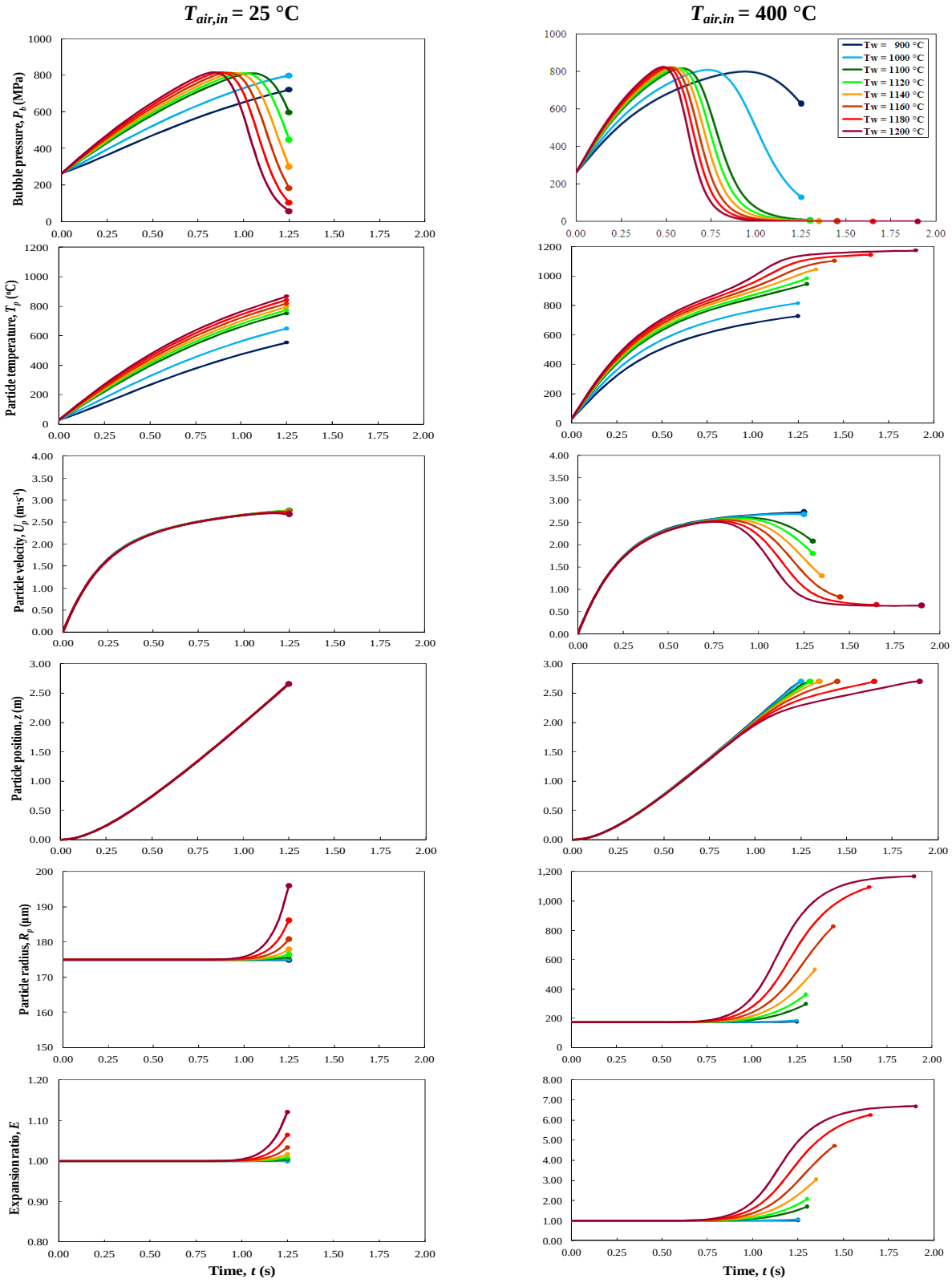

Figure 5. Temporal evolution of particle state variables as a function of heating chamber wall temperature, for the two air feed temperature extremes. Constant parameters: $Q_{air,in}$ = 50 L·m^{-1}, D_{pi} = 350 μm, $w_{H2O,eff}$ = 2.00%.

Figure 6 presents the effect of particle effective water content on final particle expansion ratio ($E = R_{p,\,final} / R_{p,i}$). Effective water content is critical for expansion evolution as it increases bubble pressure and decreases molten shell viscosity: hence, the higher the initial effective water content, the more efficiently perlite grains expand. The upper expansion ratio approximates E_{max} = 7, indicating that there is a global size increase limit in all cases. Moreover, preheated air injection favours particle expansion by increasing the heating chamber air temperature. Finer perlite ore fractions (150-250 μm) achieve expansion even with ambient (more so with preheated) air feed, while for coarser fractions (350-450 μm) air feed preheating as well as high furnace heating is clearly essential. High effective water content facilitates perlite processing at intermediate furnace temperatures (1000-1100 °C), implying that procuring high-quality feedstocks is imperative towards ensuring long, viable furnace operation. Nevertheless, simulation data clearly indicate that perlite expansion efficiency increases dramatically towards the maximum wall temperature, since furnace operation is most effective within the T_w = 1100-1200 °C range.

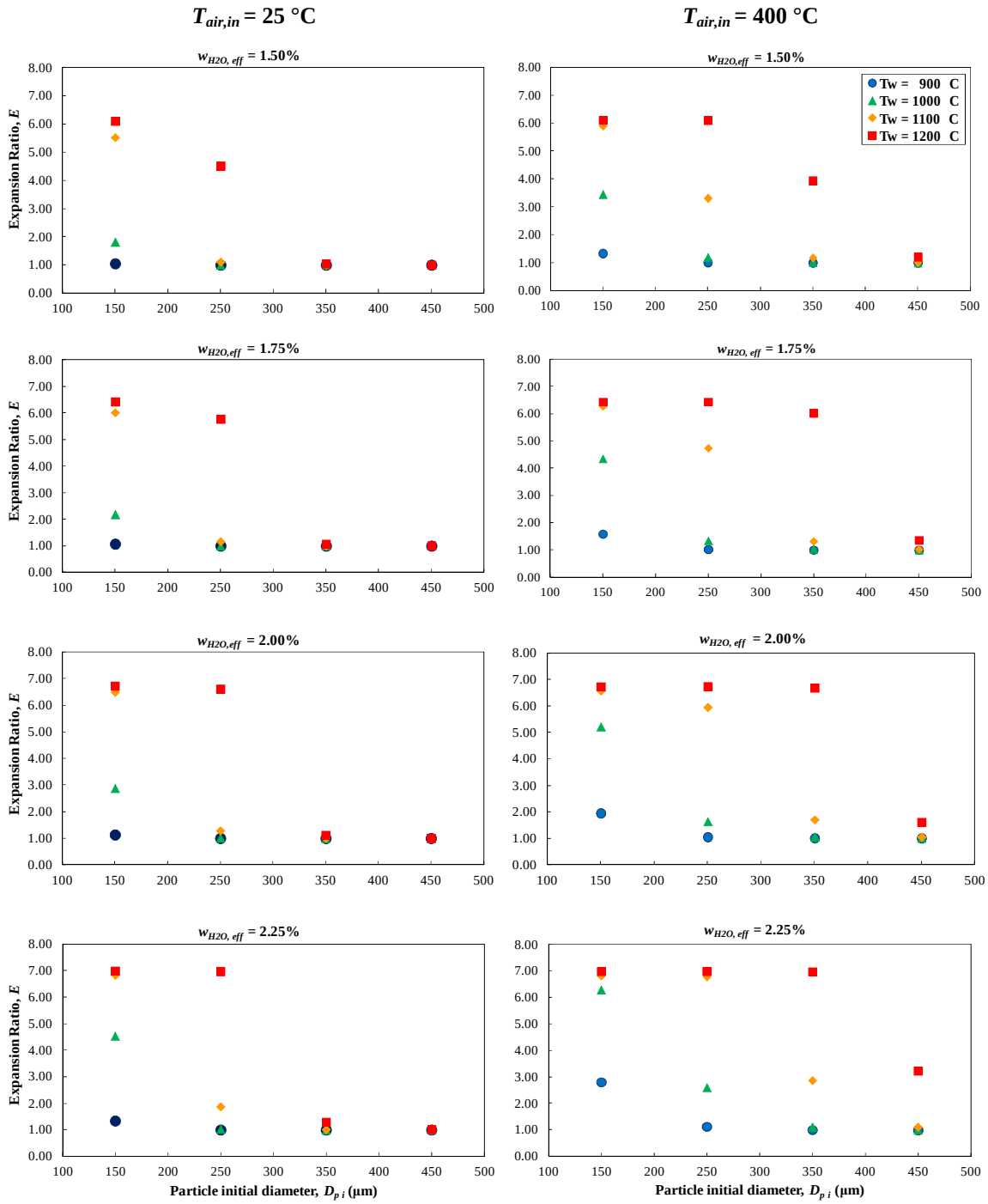

Figure 6. Final perlite particle expansion ratios achieved as a function of the initial particle diameter considered, for the entire heating chamber wall temperature and effective water content ranges. Air feed: $Q_{air,in}$ = 50 L·min^{-1}.

Figure 7 presents the effect of initial particle size on the final particle expansion ratio for various temperatures, confirming that initial perlite grain diameter (thus feedstock size distribution) is a critical expansion parameter. Finer fractions expand much easier than coarser fractions when treated under identical operating conditions: although finer grains expand even at T_w = 900 °C, larger grains require T_w > 1100 °C for sufficient expansion. Particle heating and expansion efficiency increases for decreasing size, if the minimum residence time is met. Even for finer grains though, air preheating increases process efficiency by lowering heat input requirements, so economic viability may be improved spectacularly, e.g. by an air feed heat exchange vs. the furnace air outlet. Ensuring a fine feed by sieving and coarse fraction preprocessing improves furnace productivity and efficiency considerably; however, perlite feed preprocessing should never exceed the critical perlite dust lower limit, so as to avoid disintegration phenomena because of premature radial drift, grain melting, sticking and wall fouling.

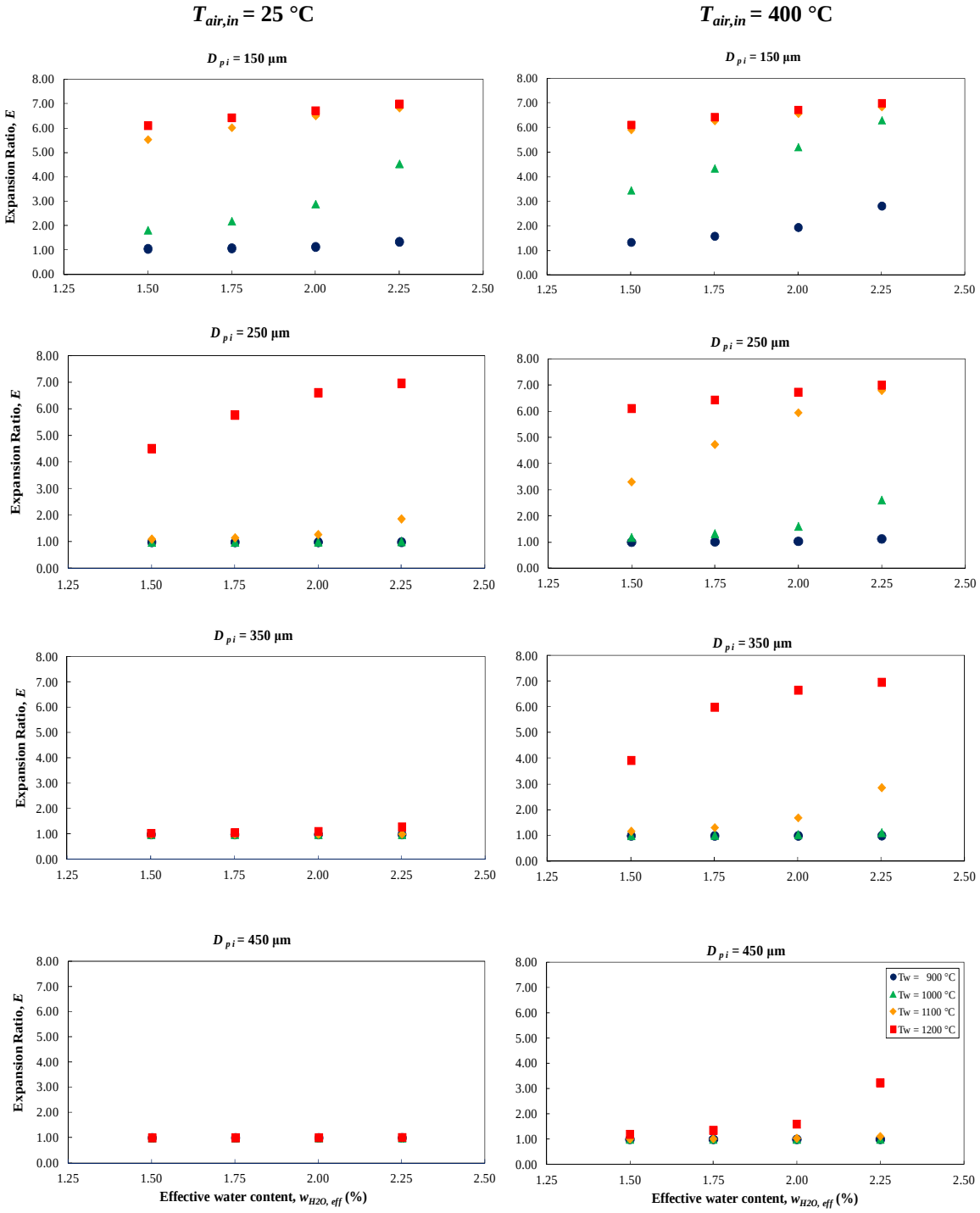

Figure 7. Final perlite particle expansion ratios achieved as a function of the effective water content considered, for the entire heating chamber wall temperature and initial particle diameter ranges. Air feed: $Q_{air,in}$= 50 L·min^{-1}.

6 CONCLUSIONS AND RECOMMENDATIONS

A mathematical model has been developed for perlite grain expansion within a novel vertical electrical furnace. This dynamic model consists of ordinary differential equations for both air and particle heat and momentum balances, as well as nonlinear algebraic equations for air and perlite melt thermophysical properties, probing air as well as particle momentum and heat balances and their effect on perlite acceleration, heating and expansion. The particle heat balance considers heat transfer by convection from/to air and by incident thermal radiation emitted by the internal chamber wall surface, which is heated via independent embedded electrical resistances. The two-phase perlite particle assumption considers an initially miniscule core bubble and an amorphous shell: the entire portion of water available for evaporation is concentrated in the core bubble (effective water content), while the rest is homogeneously dissolved in the melting shell surrounding the bubble (residual water content). The model computes the evolution of all key particle state variables (i.e. bubble pressure, particle temperature, particle velocity, particle position, particle radius and expansion ratio) and the air temperature distribution in the furnace, allowing the detailed investigation of the perlite expansion method towards cost-effective optimization. Process operating parameter (furnace wall temperature, air feeding rate, air feed temperature) and raw material physical property variations (particle water content, initial particle diameter) have been considered as dynamic model input parameters, in order to probe their process significance and relative effect on expansion efficiency by quantitatively determining their individual effect on particle expansion ratio (the key product quality metric).

The major conclusion of this modeling study is that the novel vertical electrical furnace design can successfully accomplish perlite expansion up to final product quality standards, within an acceptably wide operating regime. The new vertical electrical furnace enables the precise control of three different process operating parameters (air feed flow rate, air feed temperature, furnace wall temperature) which must be adjusted simultaneously, with in-depth, model-based (not experiential) process understanding in order to tune perlite expansion successfully. Both furnace operating conditions and feed thermophysical properties strongly impact expanded perlite quality, as shown by model results probing the entire system operating parameter ranges for two Milos mine ore feeds.

Raw perlite feedstock thermophysical properties affect perlite expansion efficiency dramatically, indicating that vertical electrical furnace tuning has paramount importance to ensure expansion for variable feed grade quality. Figures 6 and 7 corroborate quantitative observations derived from novel furnace experimental campaigns: the expansion ratio is strongly dependent on initial particle diameter as well as ore origin and chemical composition. Dynamic modeling results imply feed monodispersity is an ideal prerequisite for high-quality perlite production; in practice, optimal operating parameters vary and should be a priori determined for varying perlite ore feeds, especially when production-scale units process batches of widely varying origin and particle size distribution. Technical efficiency and economic viability can be maximized by consistent ore feed testing and preprocessing.

A key process parameter is the perlite ore feed quality, as it directly affects particle motion as well as heating. The feed particle size distribution ($D_{p,i}$) bears high importance and should ideally be narrow and monodisperse. Feeds consisting of various size fractions yield poor product quality, due to the wide variety of expansion ratios. Finer particles move slower than coarser ones, because their lower initial mass and radius impact the interplay of weight, drag and buoyancy forces towards inducing a lower terminal velocity in comparison to coarser grains. The short residence time computed for coarse grains in the furnace implies heating rates may be inadequate, so expansion may not commence or conclude due to the unfavourable interplay of gravity, shape and air injection. Moreover, a higher particle mass implies a higher heat amount required to increase its enthalpy and temperature. The total (inlet-to-outlet) particle temperature increase may thus be insufficient, causing a low expansion ratio. Residence time is crucial for coarser particles, whose terminal velocity is higher than that of finer particles: as they travel quicker and contain more water, adequate heating, softening and expansion may not occur until exit. This definite difficulty in expanding coarser particles has been observed experimentally in the vertical furnace: however, it can be effectively overcome by decreasing the air feed flow rate and/or increasing its temperature. Both these control manipulations increase particle residence time and air temperature in the heating chamber.

Optimal operating conditions strongly depend on perlite ore, so quality control and preprocessing is advisable. Common industrial practice avoids feed screening, since narrowing the feed particle size distribution inevitably raises process cost; mixing feeds from different ore mines is also very rare due to the increased uncertainty. Currently, when the feed is characterised by a wide size distribution, a mean particle diameter is determined and the feed is processed under the optimal conditions corresponding to the mean particle diameter and composition. The existence of unexpanded and shattered particles in the expanded perlite product is thus inevitable; however, post-process quality control ensures the commercial product meets the desired expanded perlite specifications.

Effective water content ($w_{H2O,eff}$) is another feed physical property affect perlite expansion and final grain size. The important distinction made in our model between residual and effective water in each perlite grain has been motivated by mass balance results from LOI tests we have conducted for both raw and expanded perlite grains. The water content in the particle is thus distinguished into the effective (bubble) and the residual (melt) portion, affecting both bubble dynamics as well as shell viscosity, which is the pivotal melt thermophysical property. Particles with more water tend to expand to higher ratios, even under mild heating (lower furnace temperatures). A higher shell water content induces quicker melt viscosity reduction, thereby facilitating rapid grain expansion. Increasing grain water content also implies a larger bubble mass as well as increased steam pressure exerted on the bubble-shell interface, thus increasing the driving force for grain expansion and improving process potential. Low-water content perlite ore feeds can therefore be processed by allowing for a longer particle residence time, through decreasing the air feed flow rate and/or increasing the furnace wall temperature and heating intensity. The maximum final particle expansion ratio achieved for adequately high effective water content ($w_{H2O,eff} > 2\%$) is almost independent of initial perlite grain diameter and model simulations indicate it does not exceed $E_{max} = 7$.

Air feed flow rate ($Q_{air,in}$) is an operating parameter which requires further numerical investigation, as this study confirms its high impact and control potential, both on the particle momentum as well as on the air heat balance. Air injection reduces residence time and can be used for restricting (ambient) or enhancing (hot) heat transfer. Finer ore feeds containing small particles ($D_{p,i} \leq 250$ μm) expand sufficiently and independently of air feed rate, as long as the operating furnace wall temperature exceeds 1100 °C along the entire heating chamber height: here air injection is not necessary, but can be quite useful against overheating and disintegration of ultrafine particles. Coarser ore feeds with large particles ($D_{p,i} > 250$ μm) must be treated at low air feed flows ($Q_{air,in} < 50$ L·min^{-1}), regardless of whether ambient or preheated air is used in order to promote particle acceleration and expansion: here, air injection is essential towards intense heat transfer throughout flight, without deteriorating side-effects. Thus, air feed must be adjusted to ensure the optimal particle residence time but also guard against reducing the air temperature inside the heating chamber, implying that volumetric air feed rate is a key optimization variable. Consequently, dynamic air feed flow rate adjustment is a very likely requirement for raw perlite grade variation.

Preheated air injection is crucial in achieving adequate perlite heating and commercially acceptable expansion, by providing a more uniform driving force for particle heating and thereby enhancing process controllability. Air feed temperature ($T_{air,in}$) affects the heating chamber temperature profile and particle temperature evolution. In all cases of large initial mean diameter ($D_{p,i} > 0.5$ mm) and/or polydispersity of perlite ore feed, ambient air use is a very poor processing choice, as it results either in no expansion or in unacceptably low product quality. The effect is stronger for coarse particles, but independent of grain water content and furnace wall temperature.

Furnace wall temperature (T_w) is of paramount importance and affects grain expansion evolution dramatically. Particle expansion is almost never observed when the furnace operates at low wall temperature ($T_w = 900$ °C), implying high-temperature operation ($T_w > 1000$ °C) is essential towards observable expansion of perlite grains; moreover, when increasing the furnace wall temperature ($T_w > 1100$ °C), higher expansion ratios are achieved. The impact of furnace wall temperature on particle expansion ratio (E) is evident in the 1100-1200 °C range, thus motivating a focused investigation of furnace operation at a higher resolution (20 °C increments) therein. Model results indicate process efficiency increases considerably at high power input; for certain quality cases, the particle expansion ratio increases up to 6 times when the furnace wall temperature increases only by 100 °C. The furnace wall temperature is an effective (albeit costly) manipulation variable, enhancing process potential.

A critical process design consideration is the heating chamber (and the entire vertical electrical furnace) height. When particle heating is inefficient, increasing the total particle trajectory length increases its residence time, thereby its exit temperature: the critical grain point and an acceptably high expansion ratio can thus be attained. Increased furnace height obviously enables successful processing of even coarser ($D_{p,i} > 450$ μm) feed fractions, as a longer flight path guarantees the required particle residence time, thereby adequate heating and expansion. Excessive overdesign must be avoided though, to elude the risk of finer fraction overheating and disintegration. The effect of vertical furnace diameter on final product quality and process efficiency also merits investigation, although it appears secondary in comparison to the pivotal effect of heating chamber height (particle trajectory length). Nevertheless, furnace diameter affects the established air flow pattern inside the heating chamber and its value certainly affects the intensity of particle swirling, collision, aggregation and sticking phenomena; the latter are known to induce gradual wall fouling and efficiency decline, as witnessed after our experimental campaigns. Consequently, future research efforts on solving the integrated vertical electrical furnace design problem must recognize and explicitly model both heat transfer and flow effects (vertical acceleration and radial swirling) and their relative magnitude, in order to prevent column clogging while avoiding overdesign and wasteful operation. Experimental measurements and visual intervention (autopsies) before and after perlite expansion tests should preferably complement dynamic simulation towards exploring the acceptable envelope of operating conditions.

ACKNOWLEDGEMENTS

This work has been financed by the European Union Seventh Framework Programme (project CP-IP 228697-2, Efficient exploitation of EU perlite resources for the development of a new generation of innovative and high added value micro-perlite based materials for the chemical, construction and manufacturing industry, EXPERL). Mr. P. Angelopoulos would like to also acknowledge the financial support of the Greek Scholarship Foundation.

REFERENCES

[1] Angelopoulos, P.M., Gerogiorgis, D.I., Paspaliaris, I. (2012), "Mathematical modeling and simulation of perlite grain expansion in a vertical electrical furnace". *Proceedings of the 5th International Conference from Scientific Computing to Computational Engineering*, Athens, Greece, pp. 331-338.

[2] Chatterjee, K.K. (2008), *Uses of Industrial Minerals, Rocks and Freshwater*. Nova Science Publishers, New York, USA.

[3] Papanastassiou, D.J. (1979), "Perlite expansion in a vertical furnace – A simplified theoretical analysis". *Proceedings of the Perlite Institute Annual Meeting*, Dubrovnik, Yugoslavia, pp. 67-71.

[4] King, E.G., Todd, S.S., Kelley, K.K. (1948), "*Perlite thermal data and energy required for expansion*" United States Bureau of Mines.

[5] Shackley, D. (1988), *Characterization and Expansion of Perlite*, PhD Thesis, Univ. of Nottingham, UK.

[6] Zahringer, K., Martin, J.-P., Petit, J.P. (2001), "Numerical simulation of bubble growth in expanding perlite", J. Mater. Sci., Vol. 36, pp. 2691-2705.

[7] Proussevitch, A.A, Sahagian, D.L. (1998), "Dynamics and energetics of bubble growth in magmas: Analytical formulation and numerical modeling", J. Geophys. Res., Vol. 103, pp. 18223-18252.

[8] Giordano, D., Russell, J.K., Dingwell, D.B. (2008), "Viscosity of magmatic liquids: A model", Earth Planet Sc. Lett., Vol. 271, pp. 123-134.

[9] Vogel, D.H. (1921), "Temperaturabhängigkeitsgesetz der Viskosität von Flüssigkeiten", Z. Phys. Chem., Vol. 22, pp. 645-646.

[10] Fulcher, G.S., (1925). "Analysis of recent measurements of the viscosity of glasses", J. Am. Ceram. Soc., Vol. 8, pp. 339-355.

[11] Morsi, S.A., Alexander, A.J. (1972), "An investigation of particle trajectories in two-phase flow systems", J. Fluid Mech., Vol. 55, pp. 193-208.

[12] Liang, S.F., Zhu, C. (1998), *Principles of Gas-Solid Flows*. Cambridge University Press, Cambridge, UK.

[13] Hausen, H. (1943), *Darstellung des Warmenberganges in Rohren durch verallgemeinerte Potenzbeziehungen*, VDI Z Beihefte Verfahrenstechnik, Germany.

[14] Kanthal: www.kanthal.com/en/products/material-datasheets/tube/kanthal-apm/ (Accessed: 30/5/2012).

[15] Patel, R.D. (1980), "Bubble growth in a viscous Newtonian liquid". Chem. Eng. Prog., Vol. 35, pp. 2352-2356.

[16] Pai, V., Favelukis, M. (2002), "Dynamics of spherical bubble growth", J. Cell. Plas., Vol. 38, pp. 403-419.

[17] Elshereef, R., Vlachopoulos, J., Elkamel, A. (2010), "Comparison and analysis of bubble growth and foam formation models". Engrg. Comput., Vol. 27, pp. 387-408.